Methane and nitrous oxide from ground-based FTIR at Addis Ababa: observations, error analysis and comparison with satellite data.

Temesgen Yirdaw Berhe[1], Gizaw Mengistu Tsidu[1,2], Thomas Blumenstock[3], Frank Hase[3], and Gabriele P. Stiller[3]

[1]Department of Physics, Addis Ababa University, P.O.Box 1176, Addis Ababa, Ethiopia

[2]Department of Earth and Environmental Sciences, College of Science, Botswana International University of Technology and Science (BIUST), Priv.Bag 16, Palapye, Botswana

[3]Institute of Meteorology and Climate Research (IMK-ASF), Karlsruhe Institute of Technology (KIT), Karlsruhe, Germany.

Correspondence: T. Yirdaw Berhe (temiephys@gmail.com)

Abstract. A ground-based high spectral resolution Fourier transform infrared (FTIR) spectrometer has been operational in Addis Ababa, Ethiopia (9.01° N, 38.76° E, 2443 m a.s.l) since May 2009 to obtain information on column abundances and profiles of various constituents in the atmosphere. The vertical profiles and column abundances of methane and nitrous oxide are derived from solar absorption measurements taken by FTIR for a period that covers May 2009 to March 2013 using the retrieval code PROFFIT (V9.5). A detailed error analysis of CH_4 and N_2O retrieval are performed. Averaging kernels of the target gases show that the major contribution to the retrieved information comes from the measurement. The degrees of freedom for signals are found to be 2.1 and 3.4 on average for the retrieval of CH_4 and N_2O from the observed FTIR spectra. Methane and nitrous oxide Volume Mixing Ratio (VMR) profiles and column amounts retrieved from FTIR spectra are compared with data from the reduced spectral resolution (Institute of Meteorology and Climate Research) IMK/IAA MIPAS (Version V5R_CH4_224 and V5R_N2O_224), the Microwave Limb Sounder (MLS) (MLS v3.3 of N_2O and CH_4 derived from MLS v3.3 products of CO, N_2O and H_2O) and the Atmospheric Infrared Sounder (AIRS) sensors on board satellites. The averaged mean relative difference between FTIR methane and the three correlative instruments MIPAS, MLS and AIRS are $4.2\%, 5.8\% and 5.3\%$ in the altitude ranges of 20 to 27 km respectively. Whereas, the bias below 20 km are negative that indicates the profile of FTIR CH_4 is less than the profiles derived from correlative instruments by $-4.9\%, -1.8\% and -2.8\%$. The averaged positive bias between FTIR nitrous oxide and correlative instrument, MIPAS in the altitude range of 20 to 27 km is 7.8 % and a negative bias of -4 % in the altitude below 20 km. An averaged positive bias of 9.3 % in the altitude range of 17 to 27 km is obtained for FTIR N_2O with MLS. In all the comparison of FTIR CH_4 with data from MIPAS, MLS and AIRS sensors on board satellites indicate a negative bias below 20 km and a positive bias above 20 km. The mean error between partial column amounts of methane from MIPAS and the ground-based FTIR is -5.5% with a standard deviation of 5 % that shows very good agreement as exhibited by relative differences of vertical profiles. Thus, the retrieved CH_4 and N_2O VMR and column amounts from Addis Ababa, tropical site is found to exhibit very good agreement with all coincident satellite observations. Therefore, the

bias obtained from the comparison is comparable to the precision of FTIR measurement, which allows the use of data in further scientific studies as it represents a unique environment of tropical Africa, a region poorly investigated in the past.

1 Introduction

Methane (CH_4), nitrous oxide (N_2O) and chlorofluorocarbons (CFCs) are tropospheric species which are the main source gases to the chemical families NO_x, ClO_x, and HO_x (Jacobson, 2005). The reaction of CH_4 with hydroxyl radicals reduces ozone in the troposphere and it influences the lifetime or production of other atmospheric constituents such as stratospheric water vapour and CO_2 (Michelsen et al., 2000; Boucher et al., 2009), whereas the lifetime of N_2O is determined by its rate of UV photolysis or reaction with $O(^1D)$ (Collins et al., 2010).

Methane retrievals from near-infrared spectra recorded by the SCIAMACHY instrument on-board ENVISAT suggested unexpectedly large tropical CH_4 emissions and the impact of water spectroscopy on methane retrievals with the largest impacts in the tropics (Frankenberg et al., 2008b). The recent increasing impact of CH_4 and N_2O to global warming has also been assessed by the last AR4 IPCC report (IPCC, 2007; Sussmann et al., 2012). Nitrous oxide (N_2O) becomes the dominant ozone-depleting substance emitted in the 21st century (Ravishankara et al., 2009). In 2007 and 2008, The Infrared Atmospheric Sounding Interferometer (IASI) on-board METOP-1 observed an increase of mid-tropospheric methane in the tropical region of 9.5 $\pm$2.8 and 6.3 $\pm$1.7 ppbv yr^{-1} respectively (Crevoisier et al., 2012). Long lived compounds ascend in the tropics, across the tropical tropopause and are subsequently redistributed by the Brewer-Dobson circulation (Holton, 2004). According to the World Meteorological Organization (WMO), the 2010 report (WMO, 2010), 96 % of the increase in radiative forcing is due to the five long-lived greenhouse gases: carbon dioxide, methane, nitrous oxide, CFC-12, and CFC-11. The sources and sinks of atmospheric methane (CH_4) and its budget in the tropics are not yet well quantified and have large uncertainties due to the scarcity of measurements (e.g., Meirink et al. 2008b).

Tropics is the location where two important exchange processes in the atmosphere are taking place, the interhemispheric exchange and the entry of tropospheric air mass into the stratosphere (Petersen et al., 2010; Fueglistaler et al., 2009). The composition of a tropical atmosphere also plays a critical role in stratospheric chemistry (Solomon, 1999; IPCC, 2007). Measurements and interpretation of atmospheric trace gas composition of tropics is vital for a better understanding of the budgets, sources and sinks of trace gases in the atmosphere and their effects on atmospheric chemistry, greenhouse effect and climate changes globally. Emissions within the tropics contribute substantially to the global budgets of many important trace gases (IPCC, 2007; Frankenberg et al., 2008).

The ground-based FTIR measurement at the Addis Ababa site has been launched since 2009 in collaboration with Karlsruhe Institute of Technology, Germany to measure concentrations of various trace gases in the lower and middle atmosphere over Addis Ababa. The Addis Ababa FTIR measurements of atmospheric trace gases and their importance to understand various lower and middle atmospheric processes have been reported in a number of previous studies (Takele Kenea et al., 2013; Mengistu Tsidu et al., 2015; Schneider et al., 2015, 2016; Barthlott et al., 2017). H_2O VMR profiles and integrated column amounts from ground-based FTIR measurements of the Addis Ababa site were also compared with the coincident satellite

observations of Tropospheric Emission Spectrometer (TES), Atmospheric Infrared Sounding (AIRS) and Modular Earth Sub-model System (MESSy) model and the result confirmed reasonably good agreement (Samuel , 2014). Laeng et al. (2015) found the MIPAS CH$_4$ profiles V5R_CH4_222 below 20 to 25 km biased +14 % high. For a later and improved data version, namely V5R_CH4_224, Plieninger et al. (2016) found a positive bias between 0.1 and 0.2 ppmv. For the MIPAS N$_2$O data version

5 V5R_N2O_224, Plieninger et al. (2016) determined the bias to be between 0 and +30 ppb.

In this study, the previous work on intercomparison of ozone (Takele Kenea et al., 2013) and water vapour (Samuel , 2014) are extended to source gases CH$_4$ and N$_2$O from ground-based FTIR. Intercomparisons of vertical profiles and column amounts retrieved from solar spectra observed by the Fourier Transform Spectrometer at the Addis Ababa site with data from MIPAS, MLS and AIRS sensors on board satellites were made to assess the quality of the data derived from FTIR. The

10 observed differences between ground-based FTIR and satellite observation of CH$_4$ and N$_2$O are analysed using the statistical tools detailed in von Clarmann (2006). The measurement site and the FTIR spectrometer along with the retrieval approach will be introduced in Section 2 and the retrieved information content and spectral analysis will be discussed in Section 3. A short description of satellite measurement techniques followed by the detailed intercomparison with satellite products will be presented in Section 4 and 5 respectively. Finally, a summary and conclusions are given in Section 6.

15 ## 2 Measurement site and Instrumentation

2.1 Measurement site

The ground-based FTIR at the Addis Ababa was established to acquire high-quality long-term measurements of trace gases to understand chemical and dynamical processes in the atmosphere and to validate models and satellite measurements of atmospheric constituents. The geographic position of the observatory is 9.01° N, 38.76° E, 2443 m a.s.l. and its suitability has

20 been confirmed from the measurements of tropical stratospheric ozone, precipitable water vapour and isotopic composition of water vapour (Takele Kenea et al., 2013; Mengistu Tsidu et al., 2015; Schneider et al., 2015, 2016; Barthlott et al., 2017). Addis Ababa is a tropical high altitude observing site and as such important to understand processes near the tropical tropopause. Physical process in tropics, mainly around tropopause layer has a vital role in climate change and the general circulation of the tropical troposphere, which would control the transport of energy, water vapour and trace gases in the climate system derived

25 by the deep convection (Holton and Gettelman, 2001). Thus, the observed variation in the measurement of atmospheric trace gases would help us to understand the effects of tropical dynamics on the site. Besides, it fills gap to the scarcity of ground based measurements in tropical.

2.2 The FTIR Spectrometer and Retrieval

Fourier transform spectroscopy has been applied successfully to study trace gases in the atmosphere by examining atmospheric

30 absorption lines in the infrared spectrum from solar. Measurement of Sun's spectra at the earth surface provides information about atmospheric composition. This technique uses the Sun as a light source to quantify molecular absorptions in the atmo-

sphere and then retrieve trace gases abundance. The high-resolution FTIR Spectrometer, Bruker IFS120M upgraded with 125 M electronics, from the Bruker Optics Company in Germany was installed in May 2009 at the Addis Ababa site. This interferometer is equipped with indium-antimonide (InSb) detector, which allows the coverage of 1500-4400 cm^{-1} spectral interval. In this spectral range, large number of species that reside in the atmosphere can be detected.

5   The measured spectra have been analyzed using an algorithm that simulates the spectra and Jacobians by the line-by-line radiative transfer model PRFFWD (PRoFit ForWarD model) to produce the synthesized spectra and the vertical profiles of CH_4 and N_2O would be derived by applying a retrieval code PROFFIT (Ver95) (Hase et al., 2004). It has been developed based on semi-empirical implementation of the Optimal Estimation Method (Rodgers, 2000) to derive the VMR profiles and column amounts of multiple species. Hence, CH_4 and N_2O profiles from measured spectra in the micro windows that span a spectral range of 2400-2800 cm^{-1} have been discussed in this paper. A Tikhonov-Phillips regularization method on a logarithmic scale were used to derive the profiles. Retrieved state vector $\hat{\boldsymbol{x}}$ is related to a priori ($\boldsymbol{x}_a$) and true state vectors ($\boldsymbol{x}$) by the following mathematical expression

$$\hat{\boldsymbol{x}} = \boldsymbol{x}_a + \hat{\mathbf{A}}(\boldsymbol{x} - \boldsymbol{x}_a) + \varepsilon \tag{1}$$

where $\hat{\mathbf{A}}$ is averaging kernel matrix and ε is the measurement error. Moreover, actual averaging kernels matrix depends on several parameters including the solar zenith angle, the spectral resolution and signal to noise ratio, the choice of retrieval spectral micro windows, and the a priori covariance matrix $\mathbf{S}_a$. The elements of averaging kernel for a given altitude gives the sensitivity of retrieved profiles at which the real profile is present and its full width at half maximum is a measure of the vertical resolution of the retrieval at that altitude (Rodgers and Connor, 1990). Error estimation analysis is based on the analytical method suggested by Rodgers (2000):

$$\hat{\boldsymbol{x}} - \boldsymbol{x} = (\mathbf{A} - \mathbf{I})(\boldsymbol{x} - \boldsymbol{x}_x) + \mathbf{G}\mathbf{K}_b(\mathbf{b} - \mathbf{b}_a) + \mathbf{G}\varepsilon \tag{2}$$

The averaging kernel matrix can be defined as A = GK, $\mathbf{I}$ is the identity matrix and $\mathbf{G}$ is gain matrix that represents the sensitivity of retrieved parameters to the measurement, $\mathbf{K}_b$ the sensitivity matrix of the spectrum to the forward model parameters $\mathbf{b}$. Since we do not know the true state of the atmosphere, we can't specify the actual retrieval error but we can only make a statistical estimate of it, which is expressed in terms of a covariance matrix. The total error in the retrieved profile can be described as a combination of measurement error and forward model parameter error. It has been suggested by Rodgers (2000) to include smoothing error to the total error budget but this concept has been revised by von Clarmann (2014).

3   Information content and error analysis

3.1   Spectroscopic data and a priori profiles

In our retrieval strategy, the profiles of CH_4 and N_2O were retrieved, while the profiles of interfering species (see Table 1) were scaled. The a prior x_a for methane and the interfering species above Adiss Ababa were taken from 40 yr averages

(1980–2020) of the Whole Atmosphere Chemistry Climate Model (WACCM, Garcia et al. 2007). Similarly, the a priori nitrous oxide profile has also constructed from monthly average data available from WACCM (e.g., Tilmes et al. 2007). Whereas, the grid to be used for the Addis Ababa site is found with the WACCM mixing ratio profile data at ftp://ftp.acom.ucar.edu/user/jamesw/IRWG/2013/WACCM/V6/Addis_Ababa/ as recommended by the NDACC/IRWG (Network for the Detection of Atmospheric Composition Change Infrared Working Group). WACCM is a numerical model developed at the National Center for Atmospheric Research (NCAR). They were constructed using the averaged values from the monthly WACCM profiles for 1980-2020 time period and used for Addis Ababa FTIR CH_4 and N_2O retrievals. Daily Profiles of pressure and temperature were taken from the NCEP reanalysis are made available through the NASA Goddard Space Flight Centre auto mailer from https://hyperion.gsfc.nasa.gov/. The spectroscopic parameters were taken from the High Resolution Transmission (HITRAN) database version 2008 of N_2O, 2009 for H_2O (Rothmann et al., 2009) and the updated HITRAN 2012 for CO, CH_4, NO_2 (Rothmann et al., 2013) were used during retrieval of CH_4 and N_2O.

Both methane (CH_4) and nitrous oxide (N_2O) are well-mixed in the troposphere and their VMR decrease with height and becomes negligible with no variation above 55 km. The vertical variability of N_2O and CH_4 in the lower stratosphere is characterized by somewhat higher vertical gradient as compared to the other layers. The vertical profiles over Addis Ababa have been obtained by fitting five and four selected spectral regions for CH_4 and N_2O respectively. Spectral micro-windows used for the retrieval are selected such that the absorption features of the target species along with a minimal number of interfering absorption lines that have been adopted from different sources (Senten et al., 2008; Sussmann et al., 2011; Meier et al., 2004) are presented. Microwindows, target and interfering species used in this paper are summarized in Table 1. However, the microwindows are somehow modified for Addis Ababa FTIR site from the windows recommended by NDACC as mentioned in a result of work done Within the EU projects UTFIR (http://www.nilu.no/uftir/) and HYMN (www.knmi.nl/samenw/hymn). The main criterion for selection of thus microwindows is high sensitivity to methane and low interference from other gases. Our tests have shown that these windows are still appropriate for the Addis Ababa site. Methane and nitrous oxide vertical profiles over Addis Ababa have been obtained by fitting five and four micro windows respectively. The retrieved state vector contains volume mixing ratios of the target gas defined in 41 layers of the tropical atmospheric conditions.

PROFFIT includes various retrieval options such as scaling of a priori profile, the Tikhonov-Phillips method (Phillips, , 1962; Tikhonov, , 1963), or the optimal estimation method (Rodgers, 2000). In this study, an optimized retrieval strategy for Addis Ababa has been established for the retrieval of CH_4 and N_2O by applying it first to single spectra, as test cases, and later routinely to the full set of measurements. Part of the strategy to optimally retrieval of the total columns of CH_4 and N_2O are to search for a set of spectra micro-windows, constraint, initial guess and a priori profile are chosen in such a way that all the structures visible in the retrieved distributions originate from the measurements and are not artifacts due to any constraints. At the Addis Ababa site, we did not use the a priori covariance matrix as an optimal estimation. However, the Tikhonov-type L_1 regularization method (Sussmann et al., 2009) on a logarithmic scale is used during the retrieval of CH_4 and N_2O. The retrieval is performed on a fine vertical grid from 2.45 to 85 km and is stabilized by a first order Tikhonov constraint, $R = \alpha L^T L$, where α is the strength of the constraint and L_1 is the first order derivative (Borsdorff et al., 2014), which smooths the solution without biasing it towards the a priori profile. The parameter determines the weight of the regularization and it

Table 1. Microwindows, interfering gases and their DOFS listed in the table are used for the retrieval of VMR profiles and column amounts of CH_4 and N_2O from FTIR spectra recorded at Addis Ababa.

Gas	micro-window(cm^{-1})	interfering species	DOFs
CH$_4$	(2599.8,2600.5)		
	(2614.87,2615.4)		
	(2650.8,2651.29)	H_2O, CO_2, NO_2	2.045
	(2760.6,2761.23)		± 0.18
	(2778.22,2778.55)		
N$_2$O	(2464.2,2465.57)		
	(2486.55,2488.18)	H_2O, CO_2, CH_4	3.38
	(2491.86,2492.9)		± 0.15
	(2522.95,2524.1)		

is also important to choose appropriate to the problem. One way to fix this parameter is the L-curve method (Hansen, 1992). The regularization strength α, is determined by finding a trade-off between the number of degrees of freedom (a measure of the amount of information in methane and nitrous oxide retrieval), which is given by the trace of the averaging kernel and the noise induced error (Rodgers, 2000). A regularization strength α, of 2.5×10^4 was found optimum for CH_4 retrieval.

5   The spectral fit and residual between measured and simulated spectra at five micro windows for CH_4 is shown in Fig. 1 for spectra recorded on Feb. 26, 2013. Whereas, four micro windows are used for N_2O and depicted in Fig. 2 for spectra recorded on Dec 31, 2009. The last column of Table 1 provides typical values for the degrees of freedom for signal (DOFS) and it indicates the possible independent pieces of information of the target gases distribution. The magnitude of residuals of spectral fits span a range of a maximum of +0.25 % to -0.64 % for CH_4 and + 0.34 % to -0.34 % for N_2O which indicates systematic

10   errors in the spectroscopic line data used to derive the concentration of CH_4 and N_2O. Therefore, the fits are good with an averaged root mean square residual of 0.12 % for the micro windows selected in the retrieval of CH_4.

     The quality of the measurements during the time period of May 2009-February 2011 for ozone has been revealed by Takele Kenea et al. (2013). Whereas, the quality of the measurements for CH_4 and N_2O has also assessed through the sensitivity, DOFs and the contribution of different error sources on measurements in addition to the spectral residuals that indicate systematic

15   errors in the spectroscopic line data.

3.2   Vertical resolution and sensitivity assessment

The spectral resolution of a measurement affects the amount of vertical information derived from the spectral line shape of a measured species (Livesey et al., 2008). Figure 3 shows averaging kernel matrices for the retrieval of the vertical profiles of CH_4 and N_2O mixing ratios, respectively, from the FTIR measurements. The rows of the averaging kernel matrices at selected

20   altitudes which indicate the sensitivity of retrieved CH_4 and N_2O values at the level to true mixing ratios are also presented.
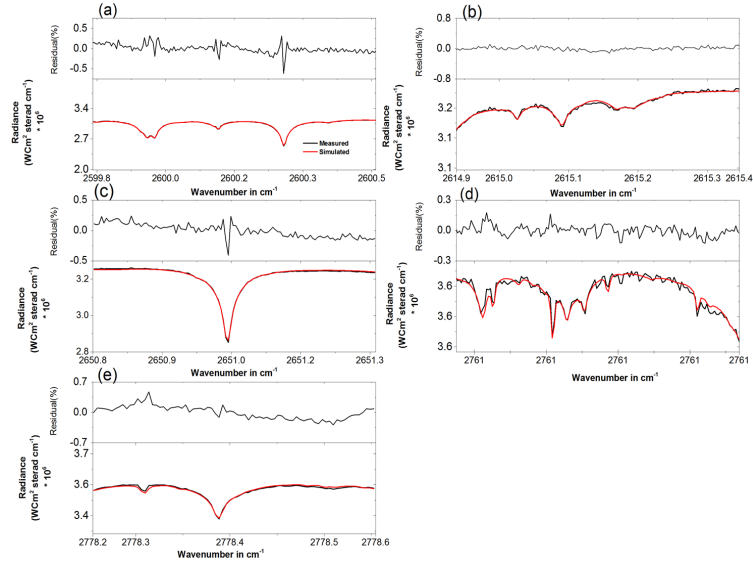
Figure 1. The five spectral micro-windows used for retrieval of CH_4, with the measured spectrum in red, simulated spectrum in black and residuals on top of the respective microwindow for spectrum recorded on Feb 26 2013, time: 10h17m15s, root mean square (RMS) =0.1189, solar zenith angle (SZA)= 20.6°, Optimal Path Difference (OPD)=116.1, DOF = 2.23, Field Of View (FOV)=2.27 mrad.
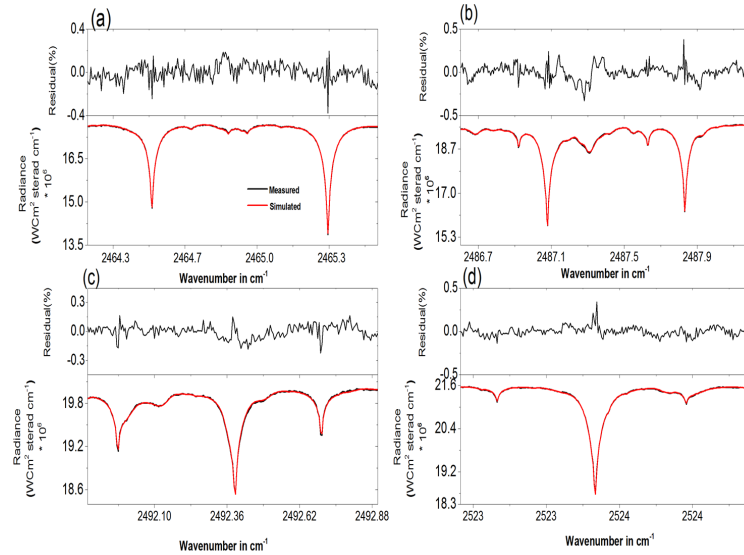
Figure 2. The four spectral micro-windows used for retrieval of N_2O, with the measured spectrum in red, simulated spectrum in black and residuals on top of the respective microwindow for spectrum recorded on Dec 31 2009, time: 09h3m727s,solar zenith angle (SZA) = 13.4°, Optimal Path Difference (OPD) =100, DOF = 3.35.

The dotted line represents the sum of all the rows of the averaging kernel, which represents the overall sensitivity of the FTIR measurement to observe CH_4 and N_2O.

Figure 3 shows a strong sensitivity in the altitude range of the troposphere and lower stratosphere , i.e. 2.45 up to 27 km for the retrieval of CH_4 and N_2O. Thus, sum of rows of **A** for all the retrieval values of CH_4 and N_2O are greater than 0.5 up to 5 27 km. The trace of the averaging kernel CH_4, which is 2.25 for the spectra recorded on Feb. 26, 2013 and 2.11 ± 0.06 for the whole data which implies that partial columns representing two different altitude ranges in the atmosphere can be obtained from the observations of CH_4 in tropical atmospheric conditions. Similarly, the trace of the averaging kernel N_2O is 3.38 ± 0.15 for the whole data.

The amplitude of the averaging kernels indicates the sensitivity of the retrieval and the full widths at half maximum (FWHM) 10 indicate the vertical resolution of the corresponding layer. We also ignore the altitude range were the resolution of the instrument becomes beyond 20 km, which has been computed using the reciprocal of the diagonal values of averaging kernels and multiplying by the intervals of the layers as reported in Rinsland et al. (2005). The vertical resolution is less than 20 km for the altitude below around 27 km (not shown).
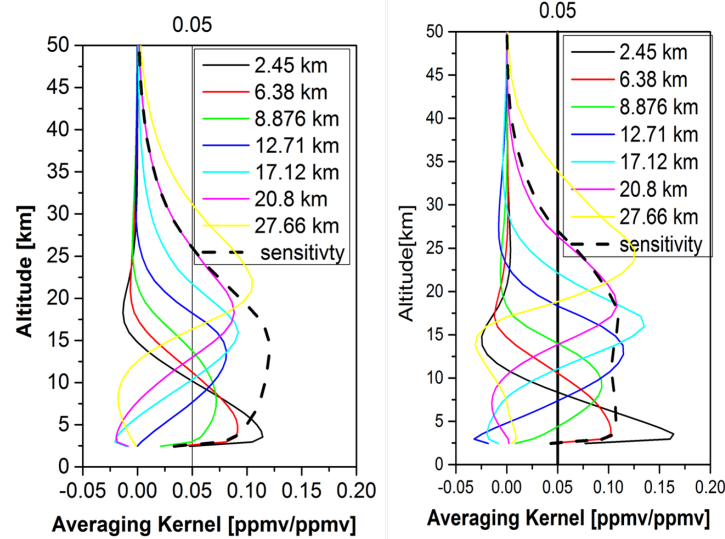
Figure 3. Sensitivity analysis of the retrieved profiles of CH_4 (left) and N_2O (right) at Addis Ababa using the selected rows of the averaging kernels as a function of altitude. The dotted lines are the sum of the rows of averaging kernels for a spectrum measured on Feb. 26, 2013 for CH_4 and Dec 31, 2009 for N_2O.

3.3 Error estimation

The error calculations conducted here are based on the error estimation package incorporated in the PROFFIT retrieval algorithm that was developed based on the analytical method suggested by Rodgers (2000). The quantified sources of errors are temperature, measurement noise, instrumental line shape, solar lines, line of sight, zero level baselines offset, and spectroscopy. It has been observed that baseline and atmospheric temperature uncertainties are the leading contribution to the total uncertainty. Details about the evaluation of the individual contributions to the error budget are provided in Senten et al. (2008). Figure 4 shows the statistical (random) error, systematic error and total fractional error (left to right) for CH_4 (top) and N_2O (bottom) retrieval from a spectrum recorded on Feb. 26, 2013 and Dec. 31, 2009 respectively. It can be noted from Fig. 4 that the main systematic error source is the uncertainty of spectroscopic parameters, whereas the major statistical error source is the baseline. Random errors are dominated by the baseline offset uncertainty and the measurement noise in the troposphere. Total estimated random error due to parameter uncertainties is depicted as dark yellow line (see Fig. 4, top panel). The total statistical error of CH_4 retrieval is about 0.07 ppmv (4.4 %) in the lower troposphere and about 0.04 ppmv (2.25 %) in the UT/LS region. Concerning systematic errors, spectroscopic parameters are the dominant uncertainty sources and estimated total systematic error is about 0.05 ppmv (3.5 %) and 0.1 ppmv (7.2 %) for the lower troposphere and the UT/LS region, respectively.

Figure 4 (bottom panel) shows the estimated random and systematic errors for the N_2O profile retrieved from FTIR. Random errors are dominated by the baseline offset uncertainty and temperature in the troposphere. The total statistical errors in middle and upper troposphere are between 0.009 ppmv (3.5 %) and 0.03 ppmv (9 %) with its major contribution from the baseline. Spectroscopic parameters and baselines are the dominant uncertainty sources for systematic errors. The estimated total systematic error is less than 0.025 ppmv (8 %) in the altitude below 22 km. The total fractional error of CH_4 and N_2O retrieved from ground-based FTIR has been shown in the last column of Fig. 4. Fractional error of CH_4 is less than 10 % in the altitude below 27 km with minimum fractional error of 4 % at middle troposphere. On the other hand, the total fraction error of N_2O retrieval is less than 13 % in the altitude below 27 km with a minimum value of 4 % at 6 km and 7.5 % at 17 km.

Time series partial Column amount

Concentrations of CH_4 and N_2O were derived from 166 spectra of NDACC filter 3 recorded from May 2009 to March 2013. Figure 5 shows the time series of the retrieved total column amounts (in molecules cm^{-2}) of CH_4 and N_2O obtained from the Addis Ababa FTIR measurement site from 2009-2013. The mean total column amounts of CH_4 and N_2O measured at Addis Ababa are 2.9×10^{19} molecules $cm^{-2}\pm3.4$ % and 5.23×10^{18} molecules $cm^{-2}\pm6.93$ %, respectively. Due to sensitivity of the observation in measuring CH_4 and N_2O trace gases is limited to an altitude of around 27 km as explained using averaging kernel row of the measurement, the mean partial column of CH_4 and N_2O within the sensitivity range of the instrument are determined as 2.85×10^{19} molecules $cm^{-2}\pm5.3$ % and 5.16×10^{18} molecules $cm^{-2}\pm6.95$ %, respectively. The sensitivity, from the averaging kernel analysis is used to determine the upper altitude limit up to which CH_4 and N_2O data from ground-based FTIR can reasonably be used. The DOFS within these partial columns limits are about 1.03 for CH_4 and 1.27 for N_2O. Error analysis indicates that the statistical error accounts for 2.3 % in the total column amounts of CH_4 and 2.0 % in total columns
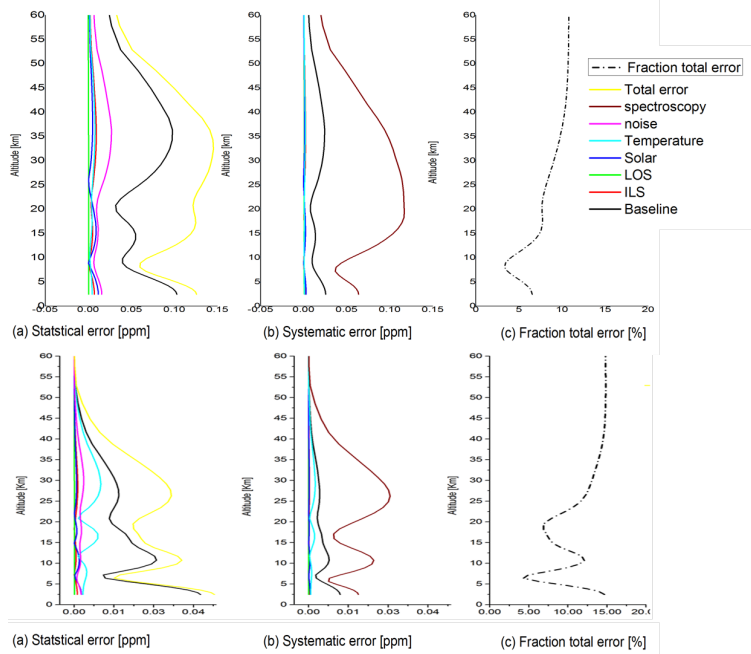
Figure 4. Estimated errors for the profiling retrieval of CH_4 (Top) and N_2O (bottom) over Addis Ababa: (a) statistical (random) errors (b) systematic errors of parameter listed in the legends, (c) Fractional total error [%].

of N_2O. Similarly, the systematic error accounts for 2.1 % in total column of CH_4 and 2.26 % in the total columns of N_2O. Generally, the overall contribution of both statistical and systematic errors to the total error during the retrieval of CH_4 and N_2O from ground-based FTIR are 3.1 % and 3 % respectively.

4 Satellite measurements

4.1 Michelson Interferometer for Passive Atmospheric Sounding (MIPAS)

Michelson Interferometer for Passive Atmospheric Sounding (MIPAS) is a Fourier transform spectrometer for the detection of limb emission spectra from the upper atmosphere to the lower thermosphere and designed for global vertical profile measurement of many atmospheric trace constituents relevant to the atmospheric chemistry, dynamics, and radiation budget of the middle atmosphere. The vertical resolution of MIPAS ranges from 2.5 to 7 km for CH_4, and from 2.5 to 6 km for N_2O in the reduced-resolution period (Plieninger et al., 2015). In this study, we have used the reduced spectral resolution (Institute of Meteorology and Climate Research) IMK/IAA MIPAS methane and nitrous oxide data product V5R_CH4_224 and V5R_N2O_224 (Plieninger et al., 2016, 2015). MIPAS profile points, where the diagonal element of the averaging kernels above 0.03 and the visibility flag of 1 have been used (Plieninger et al., 2016).
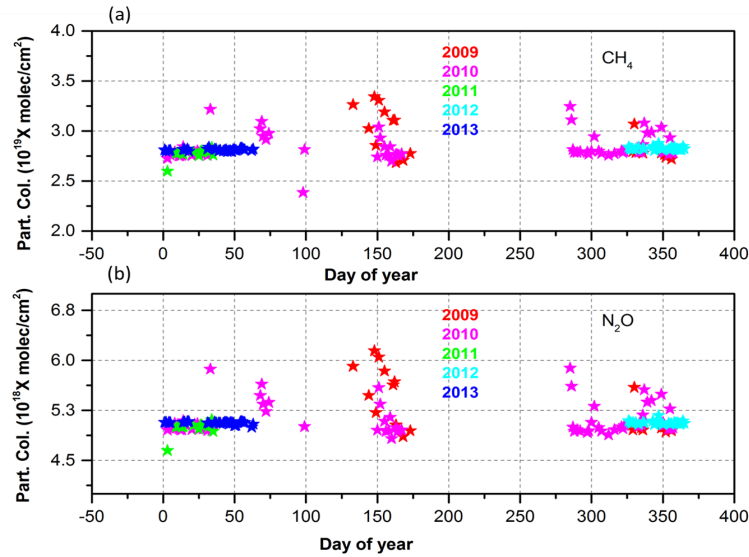
Figure 5. Partial columns of CH_4 (top) and N_2O (bottom) gases over Addis Ababa in the altitude range of 2.45 to 27 km.

4.2 Microwave Limb Sounder (MLS)

The Earth Observing System (EOS) Microwave Limb Sounder (MLS) is one of four instruments on the NASA's EOS Aura satellite, launched on July 15, 2004 into a near polar sun-synchronous orbit at 705 km altitude (Schoeberl et al., 2006). It measures N_2O in spectral region, 640 GHz from the stratosphere into upper troposphere (Waters, 2006). Moreover, spatial

5   coverage of this instrument is nearly global (-82° S to 82° N) and individual profile spaced horizontally by 1.5° or 165 km along the orbit track. Roughly the satellite covers this latitudinal bands with 15 orbits per day or around 3500 vertical profiles per day. The vertical resolution is between 4 to 6 km for N_2O. This instrument ascends equatorial region at local time of around 13:45 hour.

     MLS N_2O data set has been used to validate the ground-based FTIR measurements. However, methane (CH_4) data are

10   derived using coincident measurements of atmospheric water vapor (H_2O), carbon monoxide (CO) and nitrous oxide (N_2O) from the EOS MLS instrument on the NASA Aura satellite and detail are given in Minschwaner et al. (2015). Selection criteria were implemented as stated in Livesey et al. (2013). More details regarding the MLS experiment and data screening are provided in the above references in detail and at $http://mls.jpl.nasa.gov/data/datadocs.php$. MLS N_2O v2.2 has been validated and its precision and accuracy is respectively in Lambert et al. (2007). The authors reported that MLS N_2O precision

15   is 24-14 ppbv (9-41 %) and the accuracy is 70-3 ppbv (9-25 %) in the pressure range 100-4.6 hPa.

4.3 Atmospheric Infrared Sounder (AIRS)

Operating in nadir sounding geometry, the Atmospheric Infrared Sounder (AIRS) on board the Aqua satellite launched into Earth orbit in May 2002 Chahine et al. (2006). AIRS is a medium-resolution infrared grating spectroradiometer and a diffraction grating disperses the incoming infrared radiation into 17 linear detector arrays comprising 2378 spectral samples. The satellite crosses the equator at approximately 1:30 A.M. and 1:30 P.M. local time, resulting in near global coverage twice a day. AIRS 2378 channels covers from 649 to 1136, 1217–1613 and 2169–2674 cm^{-1}. It also measures trace gases such as O_3, CO and to some extent CO_2. AIRS CH_4 and N_2O retrievals have been characterized and validated by Xiong et al. (2008) and Xiong et al. (2014) respectively.

5 Comparison of FTIR with MIPAS, MLS and AIRS observations

5.1 Comparison methodology

The quality of the FTIR CH_4 and N_2O for a period that covers May 2009 to March 2013 is assessed through comparison with data from MIPAS (May 2009 to December 2010), MLS (May 2009 to March 2013) and AIRS (May 2009 to March 2013) sensors on board satellites. MIPAS, MLS and AIRS retrievals were used after averaging data obtained within coincident criteria of $\pm 2°$ of latitude and $\pm 10°$ of longitude from the ground-based FTIR site in Addis Ababa and within time difference of ± 24hr. The more stringent latitudinal criterion has proven to be a good choice for all comparisons, since latitudinal variations are, in general, more pronounced than longitudinal ones Takele Kenea et al. (2013). These criteria yielded 29, 77 and 118 days of coincident measurements between FTIR and MIPAS, MLS and AIRS respectively.

The ground based FTIR measurements of CH_4 and N_2O have been validated at different locations (e.g. Senten et al. (2008)). The satellite datas (MIPAS, MLS and, AIRS) have a considerably better vertical resolution than ground-based FTIR profiles due to observation geometry, spectral windows and measurement techniques. Thus, analysis of the comparison between volume mixing ratio values derived from FTIR and MIPAS were performed for the data sets collected on May 2009 to December 2010. Furthermore, the comparison of FTIR (CH_4 and N_2O) with a MLS (CH_4 and N_2O) and AIRS (CH_4) for the time period of May 2009 to February 2013 has also applied to assess quality of the data derived from FTIR. Hence, the profiles from MIPAS, MLS and AIRS have been smoothed to make a comparison with FTIR as satellite observations attain better vertical resolution. Therefore, the satellite measurement profiles are smoothed using the FTIR averaging kernels of individual species obtained from the ground based FTIR retrieval by applying the procedures reported in Rodgers and Connor (2003) and given as

$$\mathbf{x}_{si} = \mathbf{x}_a + \mathbf{A}(\mathbf{x}_i - \mathbf{x}_a) \tag{3}$$

where $\mathbf{x}_{si}$ is the smoothed profile, $\mathbf{x}_a$ and $\mathbf{A}$ represents the a priori and averaging kernel for CH_4 and N_2O obtained from the ground-based FTIR instrument respectively and $\mathbf{x}_i$ is the initial retrieved profile obtained from satellite measurements after we interpolated it to the FTIR grid spacing. We also calculate the following error statistics that can characterize the features of

the instruments and the parameters to be observed, such as the bias between the instruments using the difference (absolute or relative) of the daily mean profile. The absolute or relative difference at each altitude layers of a pair profile is calculated using

$$\delta_i(z) = [\text{FTIR}_i(z) - \mathbf{x}_{si}(z)] \tag{4}$$

5   The mean squares error can be expressed as

$$MSE_i(z) = \sqrt{\frac{1}{N(z)-1} \sum_{i=1}^{N(Z)} [\delta_i(z)]^2} \tag{5}$$

The mean difference (absolute or relative) for a complete set of coincident pairs of profiles obtained from the ground-based FTIR and the correlative satellites is expressed as

$$\triangle_{\text{rel}}(z) = 100(\%) \times \frac{1}{N(z)} \sum_{i=1}^{N(z)} \frac{[\text{FTIR}_i(z) - \mathbf{x}_{si}(z)]}{[\text{FTIR}_i(z) + \mathbf{x}_{si}(z)]/2} \tag{6}$$

10   where $\delta_i(z)$ is the difference (absolute or relative), $N(z)$ is the number of coincidences at z, $\text{FTIR}_i(z)$ is the FTIR VMR at z and the corresponding $\mathbf{x}_{si}(z)$ volume mixing ratio derived from satellite instruments. The standard deviation from the mean differences (absolute or relative) $\sigma_{diff}(z)$ is important to partially characterize the measurement error. As reported in von Clarmann (2006), some use de-biased standard deviation, which measures the combined precision of the instruments instead of the standard deviation of the mean differences.

15   $$\sigma_{diff}(z) = \sqrt{\frac{1}{N(z)-1} \sum_{i=1}^{N(Z)} [\delta_i(z) - \triangle_{\text{abs}}(z)]^2} \tag{7}$$

where $\delta_i(z)$ is the difference (absolute or relative) for the ith coincident pair calculated using Eq.(4). The statistical uncertainty of the mean differences (absolute or relative), which is standard error of the mean (SEM) is the quantity used to judge the statistical significance of the estimated biases and it can be expressed in terms of the standard deviation of the mean:

$$SEM(Z) = \frac{\sigma(z)}{\sqrt{N(Z)}} \tag{8}$$

20   One can also conduct the comparison of FTIR and MIPAS using partial columns obtained from both FTIR and smoothed MIPAS CH_4 and N_2O. Hence, the relative difference between ground-based FTIR and smoothed MIPAS partial columns of CH_4 and N_2O by taking into account the lower altitude limit of MIPAS observations and upper limit of ground-based FTIR sensitivity has been calculated using

$$\text{RDiff}(\%) = 100 * [\frac{(\text{PC}_{\text{FTIR}}(z) - \text{PC}_{\text{Sat}}(z))}{(\text{PC}_{\text{FTIR}}(z) + \text{PC}_{\text{Sat}}(z))/2}] \tag{9}$$

25   where PC is partial column of FTIR and the corresponding satellite measurements. Here in this paper coincidence and smoothing errors are not taken into account in the full error analysis of the comparisons between remotely sensed data sets (von Clarmann, 2006). Hence, we focus on the random uncertainties of each instrument (Combined random error) that has been used to evaluate the uncertainty of the comparison (standard deviation of the difference).

5.2 Comparison of FTIR CH$_4$

In Fig. 6 mean profiles, mean differences and estimated errors versus deviations of the difference between FTIR and MI-PAS_CH4_224 mixing ratios are shown. The comparison has been made using 29 coincident data for a time period between Nov., 2009 and Dec., 2010. Middle panel of Fig. 6 indicate a negative bias of -4.8 % at around 16 km and 2 % at 22 km.

5   Between 23 and 27 km the FTIR value is higher than MIPAS values. The difference increases with altitude increases from 23 to 27 km (4.6 %) with a maximum at 27 km. A large negative bias in FTIR CH$_4$ is obtained, i.e., FTIR CH$_4$ values are lower by 0.07 (4.8 %) to 0.04 ppmv (2.2 %).

Figure 6 (right panel) indicates that the standard deviation of the mean differences is larger than the combined random error of the two instruments throughout the altitude. For instance, it is twice the combined standard deviation in the altitude above

10   20 km and less below 20 km, which indicates the underestimation of random errors of one or both of the instruments. In addition, the overestimation of standard deviation of the difference may result from not taking all the error budget of MIPAS into account and the spatial and temporal criteria sets used to collect the coincidence data of MIPAS can create a discrepancy as well. The natural variation of the methane have also contributed to the overestimation of a standard deviation of the difference as biases vary with seasons as reported in Payan et al. (2009). Figure 7 (middle panel) shows the comparison between FTIR
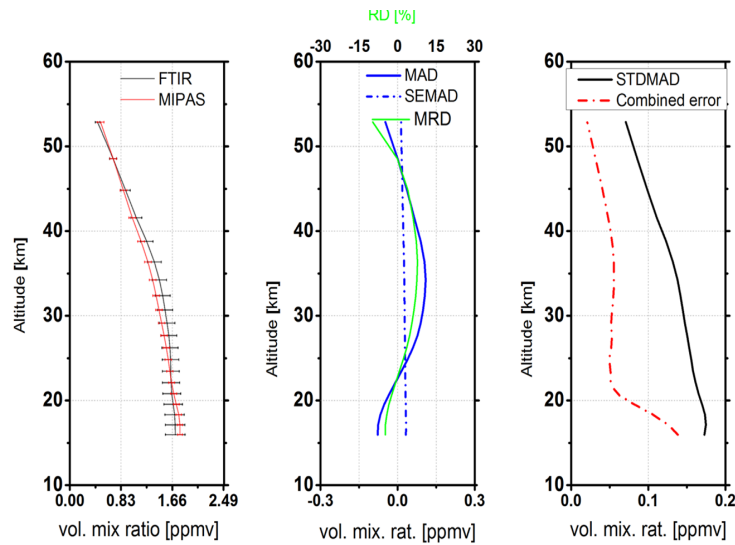
Figure 6. Comparison of CH$_4$ from MIPAS reduced resolution (V5R_CH4_224) and FTIR. Left panel: mean profiles of MIPAS (red) and FTIR (black) and their standard deviation (horizontal bars). Middle panel: mean difference FTIR minus MIPAS (MAD, blue solid), standard error of the difference (SEMAD, blue dotted), and mean relative differences FTIR minus MIPAS relative to their averaged (MRD, green, upper axis). Right panel: combined mean estimated statistical error of the difference (combined error, red dotted, contains MIPAS instrument noise error and FTIR random error budget), standard deviation of the difference (STDMAD, black solid).

15   CH$_4$ profiles and CH$_4$ derived from MLS measurements of atmospheric water vapor (H$_2$O), carbon monoxide (CO) and nitrous

oxide (N_2O) and indicates that no significant bias in FTIR CH_4 data is present between 18 and 20 km. In the tropopause layer, the comparison indicates a negative bias of -1.7 % at 17 km, i.e., the FTIR value is slightly high. FTIR CH_4 values are lower in altitude between 20-27 km with a bias of below 11 % which is maximum at 27 km or on average by 0.12 ppmv (6.7 %) between 20-27 km. The bias below 19 km and above 27 km can not be explained by the systematic errors of FTIR as the bias

5   is larger than the systematic errors of FTIR and the later is also out of the sensitivity ranges of FTIR. Furthermore, the standard deviation of the difference is larger than the combined random errors of the instruments. A bias in altitude range of 20 to 27 km can be explained by the systematic error of FTIR. In Fig. 8 mean profiles, mean differences and estimated error versus
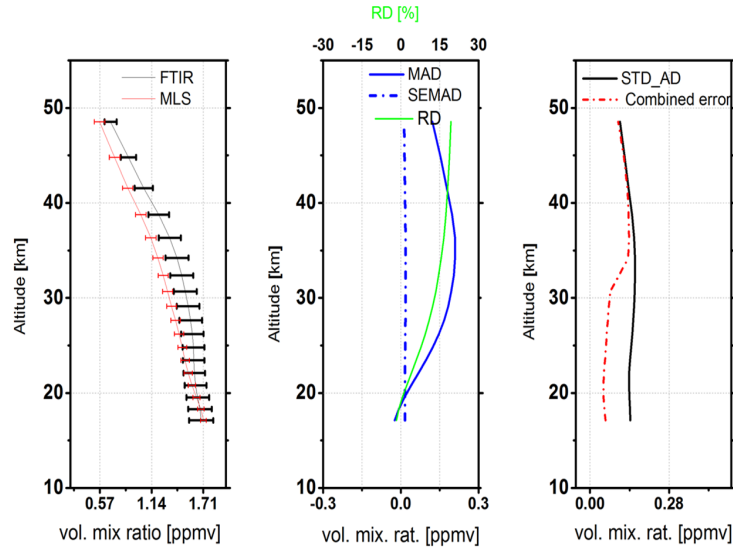
Figure 7. Comparison of CH_4 from MLS (V3.3) and FTIR. Details as in Fig. 6

deviation of the difference between FTIR and AIRS mixing ratios are shown. The largest negative bias is found in altitude between 11-19 km with a maximum difference of -0.08 ppmv at around 15 km. A negative bias that AIRS mixing ratio of CH_4

10 is higher than the FTIR as shown in Fig. 8. A positive bias existed at altitude between 7-9 km and similarly, it also shown in altitude between 21-27 km with a maximum value at around 27 km and its bias is 0.14 ppmv (9 %). The standard deviation of the difference agrees to the combined random error in altitude below 20 km and it overestimate above 20 km. In all the comparison of FTIR CH_4 with data from MIPAS, MLS and AIRS sensors on board satellites indicates a negative bias below 21 km and a positive bias above 21 km with similar bias of not higher than 5.8 % in the altitude range 21-27 km (see Table 2.).

15 The volume mixing ratios derived from the satellite are higher in altitude lower than 21 km.
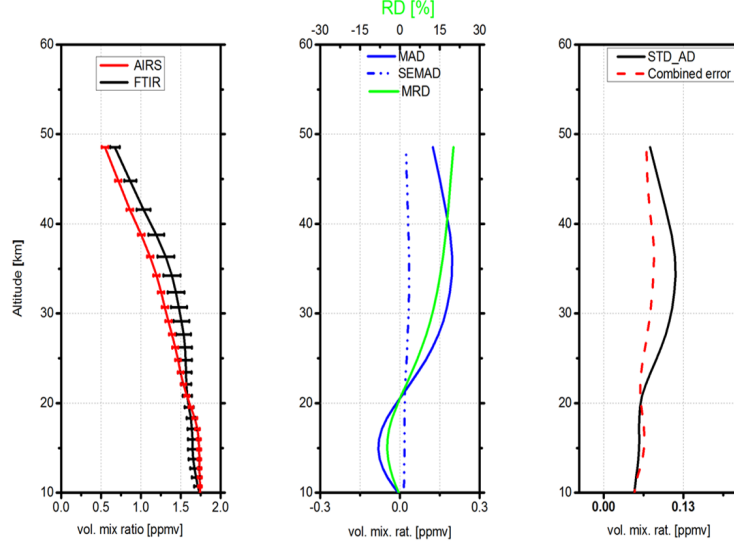
Figure 8. Comparison of CH$_4$ from AIRS and FTIR. Details as in Fig. 6

Table 2. Averaged statistical means (*M*) and standard deviations (*STD*) of the relative differences $100 * \left[\frac{FTIR-MIPAS}{\frac{FTIR+MIPAS}{2}}\right][\%]$ defined in altitude range of 17-20 km and 21-27 km. The numbers of coincidences (N) within a spatiotemporal criterion of $\pm 2°$ of latitude and $\pm 10°$ of longitude and time difference of ± 24hr are selected for intercomparison. This is for FTIR CH$_4$ and N$_2$O with the corresponding other instruments (stated in second column).

Gas	Instrument	altitude range	*M*$\pm$ *STD*	period	N
	MIPAS	17-20/21-27	-4.8/4.2 $\pm$ 5.2/5.5	May 2009-Dec 2010	29
CH$_4$	MLS	17-19/20-27	-1.8/5.8 $\pm$ 8 /8.8	Jun 2009-Feb 2013	77
	AIRS	17-20/21-27	-2.8/5.3 $\pm$ 3.5/5.4/	Jun 2009-Feb 2013	118

5.3 Comparison of FTIR N$_2$O

FTIR N$_2$O mixing ratio MIPAS comparison results are shown in Fig. 9, where it represents the mean profiles, mean absolute difference and standard deviation of the mean along with the combined errors of the two instruments. Mean profiles of FTIR show a maximum at around 23 km and decreases smoothly as altitude increases and that of MIPAS_N2O_224 value starts to decline starting from the lowermost stratosphere.

Comparison of FTIR N$_2$O profiles to MIPAS (V5R_N2O_224) measurements (see Fig. 9 (middle panel)) indicates that FTIR value is higher than the MIPAS above 20 km and the maximum mean absolute difference of N$_2$O is 15 % (0.04 ppmv) at around 24 km while, the FTIR value is less in altitude below 20 km with a maximum difference of -7 % (-0.02 ppmv) at

around 17 km. The bias at 19 km is not statistically significant as the standard error of the mean is larger than the bias. In the remaining altitudes standard error of the mean is smaller than the mean bias and the biases are statistically significant. Since, the bias in altitude between 20 to 27 km is smaller than the FTIR systematic errors, the bias could be explained in terms of systematic uncertainties in FTIR (see Fig. 4 (bottom middle panel)). The standard deviation of the difference is larger than

5   the combined error of the two instruments in the altitude above 20 km (see Fig. 9, right panel) and the standard deviation of the difference agrees with the estimated combined random error in the altitude ranges between 20 to 27 km. For the altitudes below 20 km, the estimated combined random error is overestimated.

The left panel of Fig. 10 represents the mean profiles of N_2O derived from the coincident pairs of FTIR and MLS. Throughout the whole altitude range, the value derived from FTIR is overestimated (relative to MLS). The FTIR values of N_2O are larger

10   than the MLS value of N_2O by a factor of 1.2 and 1.1 at around 21 and 27 km respectively. The mean relative difference of FTIR and MLS N_2O value increases as altitude increase, its value is less than 18.6 % in altitudes below 27 km and its bias below 22 km is less than 8 % that can be explained in terms of the systematic error of FTIR N_2O. Thus, the positive bias is statistically significant as the mean difference of the comparison is larger than the standard error of the mean.
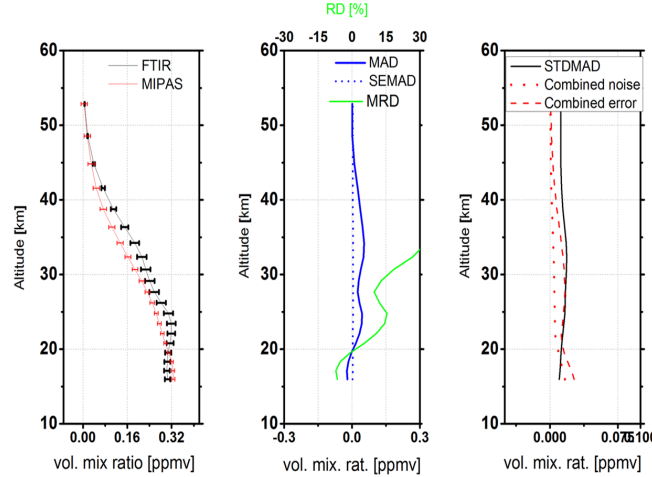
Figure 9. Comparison of N_2O from MIPAS (V5R_N2O_224) and FTIR. Details as in Fig. 6

5.4   Comparisons of partial columns

15   For the partial column (PC) comparisons of FTIR with MIPAS, it is vital to take into account the lower altitude limit of MIPAS, which is 15 km for both target gases. The ground-based FTIR sensitivity is used to determine the upper altitude limit, which is reasonable up to $\sim$ 27 km for CH_4 and N_2O in the tropical atmospheric condition. Therefore, the PC that we use in the comparison is limited to the altitude range of 15-27 km. The DOFs within these partial columns limit are about 1.0 and 1.2 for CH_4 and N_2O respectively.
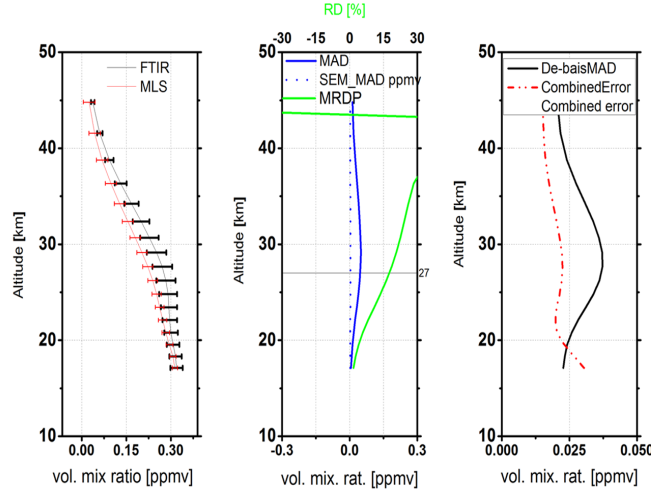
Figure 10. Comparison of N$_2$O from MLS (V3.3) and FTIR. Details as in Fig. 6

Figure 11 shows the time series of the partial columns and relative differences of CH$_4$ (upper panel) and N$_2$O (lower panel). The partial column comparison of CH$_4$ between values of FTIR and MIPAS revealed a mean error of -5.5 %, mean squares error of 7.4 % and a standard deviation from the mean error of 5 %. Similarly, N$_2$O values between FTIR and MIPAS revealed a mean error of 0.5 %, mean square error of 3.7 % and standard deviation from mean error of 3.8 % in the latter case a significant positive bias is observed and in CH$_4$ negative bias was obtained.
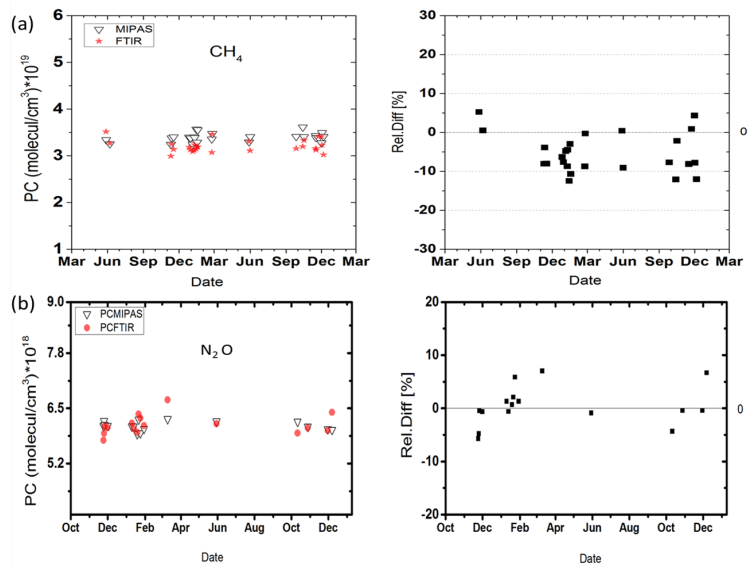
Figure 11. Time series of CH$_4$ and N$_2$O partial column comparisons for altitude range 15-27 km: right panel: ground-based FTIR (stars) and MIPAS (V5R_CH4_224 and V5R_N2O_224) (triangular) partial columns. left panel: relative differences between ground-based FTIR and MIPAS (V5R_CH4_224 and V5R_N2O_224) partial columns.

6 Summary and conclusions

The vertical profiles and partial columns of CH_4 and N_2O over Addis Ababa, Ethiopia were derived from ground-based FTIR. The mean partial column of CH_4 and N_2O within the sensitivity ranges of the instrument, which is from the surface to around 27 km is determined as 2.85×10^{19} molecules $cm^{-2} \pm 5.3$ % and 5.16×10^{18} molecules $cm^{-2} \pm 6.95$ % respectively. Furthermore, the overall contribution of both statistical and systematic errors, i.e. a total error of CH_4 and N_2O from ground-based FTIR is 3.1 % and 3 %, respectively.

From comparison of FTIR CH_4 and MIPAS_CH4_224 products, a statistically significant maximum negative bias of -4.8 % in altitude 15 km that extends to 21 km and maximum positive bias of 4.6 % in an altitude 27 km were obtained. The largest negative bias is found in an altitude between 11-19 km with a maximum difference of -0.08 ppmv (-4.8 %) at around 15 km and a positive bias of less than 0.14 ppmv (9 %) is found in altitude between 21-27 km with a maximum value at around 27 km in FTIR CH_4 comparison with AIRS. On the other hand, a comparison of CH_4 from ground-based FTIR and MLS version 3.3 indicates a significant positive average bias of 0.12 ppmv (6.7 %) in the altitude range of 20-27 km and a negative bias -1.7 % is also found at 17 km. In the case of FTIR N_2O and MIPAS_N2O_224, a significant positive bias of less than 15 % in the altitude range 22-27 km with a maximum value at around 25 km and a negative bias of -7 % at 17 km has been obtained. A positive bias of less than 18.6 % for the altitude below 27 km is noted for N_2O between FTIR and MLS and its bias below 22 km is less than 8 % that can be explained in terms of the systematic error of FTIR N_2O.

In general, the retrieved CH_4 and N_2O VMR and column amounts from Addis Ababa, tropical site is exhibited very good agreement with all coincident satellite observations in the altitude ranges of 17-27 km with a positive mean relative difference within 20-27 km and negative difference below 20 km. In addition, the bias obtained from the comparison and the precision of the FTIR measurements is also comparable. The intercomparisons of CH_4 and N_2O VMR from ground-based FTIR with data from MIPAS, MLS and AIRS sensors on board satellites reported in this work establish main features that characterise the FTIR instruments at Addis Ababa. The FTIR data can be used in further scientific studies as it represents a unique environment of tropical Africa, a region poorly investigated in the past. Furthermore, the results of this intercomparison of FTIR observations with the satellites can ensure that FTIR observations can now be used to validate satellite missions. Thus, the FTIR data is anticipated that the use of the data in further scientific studies may provide some insight into the processes that govern chemical transport and chemistry in the atmosphere as well as sources of green gases in this part of the globe.

acknowledgements

Acknowledgements. We are grateful to Goddard Space Flight Center and WACCM for providing temperature, pressure and a priori profiles of all molecules. AIRS and MLS data were obtained through the Goddard Earth Sciences Data and Information Services Center (http: //daac.gsfc.nasa.gov/). We greatly acknowledge the MIPAS science teams for providing data used in this study. Finally, authors would like to thank Mekelle and Addis Ababa universities for the sponsorship and financial support.

References

Meier, A., Toon, G. C., Rinsland, C. P., Goldman, A. and Hase, F.: Spectroscopic Atlas of Atmospheric Microwindows in the Middle Infrared; 2nd revised edition; IRF Technical Report 048 ISSN 0284-1738; Swedish Institute of Space Physics Kiruna, 2004.

Barthlott, S., Schneider, M., Hase, F., Blumenstock, T., kiel, M., Dubravica, D., Omaira, E., Sepúlveda, E., Mengistu Tsidu, G., Takele Kenea, S., Grutter, M., F. PlazaMedina, E., Stremme, W., Strong, K., Weaver, D., Palm, M., Warneke, T., Notholt, J., Mahieu, E., Servais, C., Jones, N., W. T. Griffith, D., Smale, D., and Robinson, J.: Tropospheric water vapour isotopologue data ($H_2^{16}O$, $H_2^{18}O$, and $HD^{16}O$) as obtained from NDACC/FTIR sola absorption spectra, Earth Syst. Sci. Data, 9, 15–29, doi:10.5194/essd-9-15-2017, 2017.

Borsdorff, T., Hasekamp, O, P, Wassmann, A, and Landgraf, J, : Insights into Tikhonov regularization: application to trace gas column retrieval and the efficient calculation of total column averaging kernels Atmos. Meas. Tech., 7, 523–535, doi:10.5194/amt-7-523-2014, 2014

Boucher, O., Friedlingstein, P., Collins, B., and Shine, K. P.: The indirect global warming potential and global temperature change potential due to methane oxidation, Environ. Res. Lett., 4, 044007, doi:10.1088/1748-9326/4/4/044007, 2009.

Collins, W. J., Sitch, S., and Boucher, O.: How vegetation impacts affect climate metrics for ozone precursors, J. Geophys. Res., 115, D23308, doi:10.1029/2010JD014187, 2010.

Chahine, M., Pagano, T., Aumann, H., Atlas, R., Barnet, C., Chen, L., Divakarla, M., Fetzer, E., Goldberg, M., Gautier, C., Granger, S., Irion, F. W., Kakar, R., Kalnay, E., Lambrigtsen, B., Lee, S., Marshall, J. L., McMillan, W., McMillin, L., Olsen, E. T., Revercomb, H., Rosenkranz, P., Smith, W., Staelin, D., Strow, L., Susskind, J., Tobin, D., and Wolf, W.: The Atmospheric Infrared Sounder (AIRS): improving weather forecasting and providing new insights into climate, B. Am. Meteorol. Soc., 87, 891–894, doi:10.1175/BAMS-87-7-891, 2006.

Crevoisier, C., Nobileau, D., Armante, R., Chedin, A., Scott, N. A., Pernin, J, Thonat, T. Schuck, T., Matsueda, H., Crepeau, L., Machida T., and Sawa Y.: The 2007–2011 evolution of tropical methane in the mid-troposphere as seen from space by MetOp-A/IASI, Atmos. Chem. Phys., 12, 23731–2375, doi:10.5194/acpd-12-23731-2012, 2012.

Fueglistaler, S., Dessler, A. E., Dunkerton, T. J., Folkins, I., Fu, Q., and Mote, P. W.: Tropical tropopause layer, Rev. Geophys., 47, RG1004, doi:10.1029/2008RG000267, 2009.

Frankenberg, C, Bergamaschi, P., Butz, A., Houweling, S., Meirink, J.F., Notholt, J., Petersen, A.K., Schrijver, H., Warneke, T., and Aben, I.: Tropical methane emissions: A revised view from SCIAMACHY onboard ENVISAT, Geophys. Res. Lett., 35, L15811, doi:10.1029/2008GL034300, 2008.

Frankenberg, C., Warneke, T., Butz, A., Brown, L. R., Hase, F., Spietz, P. and Aben, I.: Methane spectroscopy in the near infrared and its implication on atmospheric retrievals, Atmos. Chem. Phys. Disc., 8, 10,021–10,055, 2008b.

Garcia, R. R., Marsh, D. R., Kinnison, D. E., Boville, B. A., and Sassi, F.: Simulation of secular trends in the mid-dle atmosphere, 1950–2003, J. Geophys. Res., 112, D09301, doi:10.1029/2006JD007485, 2007.

Hansen, C.: Analysis of discrete ill-posed problems by means of the L-curve, Soc. Indust. Appl. Math., 34, 561–580, 1992.

Hase, F., Hannigan, J. W., Coffey, M. T., Goldman, A., Höpfner, M., Jones, N. B., Rinsland, C. P., and Wood, S.W.: Intercomparison of retrieval codes used for the analysis of high-resolution, ground-based FTIR measurements, J. Quant. Spectrosc. Radiat. Transfer, 87, 25-52, 2004.

Holton, J. R. and Gettelman, A.: Horizontal transport and the dehydration of the stratosphere, Geophys. Res. Lett., 28, 27992802, 2001.

Holton, J. R.: Introduction to dynamic meteorology, forth edition, Department of Atmospheric Science University of Washington, Elsevier Academic Press, 2004.

IPCC (Intergovernmental Panel on Climate Change): Third Assessment Report: Climate Change 2007: The Scientific Basis, Chapter 4, Cambridge University Press, UK, 2007.

5 Jacobson, M. Z.: Fundamentals of Atmospheric Modeling, second edition, Stanford University, Cambridge University press, 2005.

Laeng, A., Plieninger, J., von Clarmann, T., Stiller, G., Eckert, E., Glatthor, N., Grabowski, Haenel, N., Kiefer, M., Kellmann, S., Linden, A., Lossow, S., Deaver, L., Engel, A., Harvig, M., Levin, I., McHugh, M., Noel, G., and Walker, K.: Validation of MIPAS IMK/IAA methane profiles, Atmos. Meas. Tech., 8, 5251–5261, doi:10.5194/amt-8-5251-2015, 2015.

Livesey, N. J., Filipak, M. J., Froidevaux, L., Read, W. G., Lambert, A., Santee, M. L., Jiang, J. H., Pumphrey, H. C., Waters, J. W., Cofield,

10 R. E., Cuddy, D. T., Daffer, W. H., Drouin, B. J., Fuller, R. A., Jarnot, R. F., Jiang, Y. B., Knosp, B. W., Li, Q. B., Perun, V. S., Schwartz, M. J., Snyder, W. V., Stek, P. C., Thurstans, R. P., Wagner, P. A., Avery, M., Browell, E. V., Cammas, J.P., Christensen, L. E., Diskin, G. S., Gao, R. S., Jost, H.J., Loewenstein, M., Lopez, J. D., Nedelec, P., Osterman, G. B., Sachse, G. W., and Webster, C. R.: Validation of Aura Microwave Limb Sounder O_3 and CO observations in the upper troposphere and lower stratosphere, J. Geophys. Res., 113, D15S02, doi:10.1029/2007JD008805, 2008.

15 Livesey, N. J., Read, W. G., Froidevaux, L., Lambert, A., Gloria, L. Manney, H. C. P., Santee, M. L., Schwartz, M. J., Wang, S., Richard, E. Cofield, D. T. C., Fuller, R. A., Jarnot, R. F., Jiang, J. H., Knosp, B. W., Paul, C. Stek, P. A. W., and Wu, D. L.: Earth Observing System(EOS), Aura Microwave Limb Sounder (MLS), Version 3.3 and 3.4 Level 2 data quality and description document, Tech. Rep. JPL D-33509, Jet Propulsion Laboratory, California Institute of Technology, Pasadena, CA, USA, 2013.

Lambert, A., Read, W. G., Livesey, N. J., Santee, M. L., Manney, G. L., Froidevaux, L., Wu, D. L., Schwartz, M. J., Pumphrey, H. C.,

20 Jimenez, C., Nedoluha, G. E., Cofield, R. E., Cuddy, D. T., Daffer, W. H., Drouin, B. J., Fuller, R. A., Jarnot, R. F., Knosp, B. W., Pickett, H. M., Perun, V. S., Snyder, W. V., Stek, P. C., Thurstans, R. P., Wagner, P. A., Waters, J. W., Jucks, K. W., Toon, G. C., Stachnik, R. A., Bernath, P. F., Boone, C. D., Walker, K. A., Urban, J., Murtagh, D., Elkins, J. W., and Atlas, E.: Validation of the Aura Microwave Limb Sounder middle atmosphere water vapor and nitrous oxide measurements, J. Geophys. Res.: Atmospheres, 112, D24S36, doi:10.1029/2007JD008724, 2007.

25 Meirink, J. F., Bergamaschi, P., and Krol, M. C.: Four-dimensional variational data assimilation for inverse modelling of atmospheric methane emissions: method and comparison with synthesis inversion, Atmos. Chem. Phys., 8, 6341–6353, doi:10.5194/acp-8-6341-2008, 2008b.

Mengistu Tsidu G.: High resolution monthly rainfall database for Ethiopia: Homogenization, Reconstruction, and Gridding, Journal of Climate, doi: http://dx.doi.org/10.1175/JCLI-D-12-00027.1, 2012.

Mengistu Tsidu, G., Blumenstock, T., and Hase, F.: Observations of precipitable water vapour over complex topography of Ethiopia from

30 ground-based GPS, FTIR, radiosonde and ERA-Interim reanalysis, Atmos. Meas. Tech., 8, 3277–3295, doi:10.5194/amt-8-3277-2015, 2015.

Michelsen, H. A., Irion, F. W., Manney, G. L., Toon, G. C., and Gunson, M. R., : Features and trends in Atmospheric Trace Molecule Spectroscopy (ATMOS) version 3 stratospheric water vapor and methane measurements, J. Geophys. Res., 105(D18), 22713–22724, 2000.

35 Minschwaner, K., and Manney, : Derived Methane in the Stratosphere and Lower Mesosphere from Aura Microwave Limb Sounder Measurements of Nitrous Oxide, Water Vapor, and Carbon Monoxide, J. Atmos. Chem., 2015.

Petersen, A. K., Warneke, T., Frankenberg, C., Bergamaschi, P., Gerbig, C., Notholt, J., Buchwitz, M., Schneising, O., and Schrems, O.: First ground-based FTIR observations of methane in the inner tropics over several years, Atmos. Chem. Phys., 10, 7231-7239, doi:10.5194/acp-10-7231-2010, 2010.

Phillips, B. C.: A technique for the numerical solution of certain integral equations of the first kind, J. Ass. Comput. Mach., 9, 84–97, doi:10.1145/321105.321114, 1962.

Plieninger, J., von Clarmann, T., Stiller, G. P., Grabowski, U., Glatthor, N., Kellmann, S., Linden, A., Haenel, F., Kiefer, M., Höpfner, M., Laeng, A., and Lossow, S., : Methane and nitrous oxide retrievals from MIPAS-ENVISAT, Atmos. Meas. Tech., 8, 46574670, doi:10.5194/amt-8-4657-2015, 2015.

Plieninger, J., laeng, A., Lossow, S., von Clarmann, T., Stiller, G. P., Kellmann, S., Linden, A., Kiefer, M., Walker, K.A., Noel, S., Hervig, M.E., McHugh, M., Lambert, A., Urban, J., Elkins, J.W., and Mrtagh, D.: Validation of revised methane and nitrous oxide profiles from MIPAS ENVISAT, Atmos. Meas. Tech., 9, 765779, doi:10.5194/amt-9-765-2016, 2016.

Payan, S., CamyPeyret, C., Oelhaf, H., Wetzel, G., Maucher, G., Keim, C., Pirre, M., Huret, N., Engel, A., Volk, M. C., Kuell-mann, H., Kuttippurath, J., Cortesi, U., Bianchini, G., Mencaraglia, F., Raspollini, P., Redaelli, G., Vigouroux, C., De Maziére, M., Mikuteit, S., Blumenstock, T., Velazco, V., Notholt, J., Mahieu, E., Duchatelet, P., Smale, D., Wood, S., Jones, N., Piccolo, C., Payne, V., Bracher, A., Glatthor, N., Stiller, G., Grunow, K., Jeseck, P., Te, Y., and Butz, A.: Validation of version-4.61 methane and nitrous oxide observed by MIPAS, Atmos. Chem. Phys., 9, 413–442, doi:10.5194/acp-9-413-2009, 2009.

Rinsland, C.P., Boone, C., Nassar, R., Walker, K., Bernath, P., Mahieu, E., Zander, R., J.C. McConnell, J. C., and Chiou, L.: Trends of HF, HCl, CCl_2F_2, CCl_3F, $CHClF_2$ (HCFC-22), and SF_6 in the lower stratosphere from Atmospheric Chemistry Experiment (ACE) and Atmospheric Trace Molecule Spectroscopy (ATMOS) measurements near $30°$ N latitude, Published in GEOPHYSICAL RESEARCH LETTERS, VOL. 32, 22 June 2005.

Rodgers, C. D., Characterization and error analysis of profiles retrieved from remote sounding measurements, J. Geophys. Res. 95,55875595, 1990.

Rodgers, C. D.: Inverse Methods for Atmospheric Sounding: Theory and Practise, vol. 2 of Series on Atmospheric, Oceanic and Planetary Physics, World Scientific (publisher), 2000.

Rodgers, C. D. and Connor, B. J.: Intercomparison of remote sounding instruments, J. Geophys. Res., 108(D3), 4116, doi:10.1029/2002JD002299, 2003.

Ravishankara, A. R., Daniel, J. S., and Portmann, R. W.: Nitrous oxide (N_2O): The dominant ozone-depleting substance emitted in the 21st century, Science, 326, 123–125. DOI: 10.1126/science.1176985, 2009.

Rothman, L. S., Gordon, I. E., Barbe, A., Benner, D. C., Bernath, P. F., Birk, M., Boudon, V., Brown, L. R., Campargue, A., Champion, J. P., Chance, K., Coudert, L. H., Dana, V., Devi, V. M., Fally, S., Flaud, J. M., Gamache, R. R., Goldmanm, A., Jacquemart, D., Kleiner, I., Lacome, N., Lafferty, W., Mandin, J. Y., Massie, S. T., Mikhailenko, S. N., Miller, C. E., Moazzen-Ahmadi, N., Naumenko, O. V., Nikitin, A. V., Orphal, J., Perevalov, V. I., A. Perrin, A. P. C., Rinsland, C. P., Rotger, M., Šimečková, M., Smith, M. A. H., Sung, K., Tashkun, S. A., Tennyson, J., Toth, R. A., Vandaele, A. C., and Auwera, J. V.: The HITRAN 2008 molecular spectroscopic database, J. Quant. Spectrosc. Ra., 110, 533–572, 2009.

Rothmann L. S., Gordon, I. E., Babikov, Y., Barbe, A., Benner, D. C., Bernath, P. F., Birk, M., Bizzocchi, L., Boudon, V., Brown, L. R., Campargue, A., Chance, K., Coudert, L. H., Devi, V. M., Drouin, B. J., Fayt, A., Flaud, J. M., Gamache, R. R., Harrison, J., Hartmann, J. M., Hill, C., Hodges, J. T., Jacquemart, D., Jolly, A., Lamouroux, J., LeRoy, R. J., Li, G., Long, D., Mackie, C. J., Massie, S. T., Mikhailenko, S., Müller, H. S. P., Naumenko, O. V., Nikitin, A., Orphal, J., Perevalov, V. I., Perrin, A., Polovtseva, E. R., Richard, C.,

Smith, M. A. H., Starikova, E., Sung, K., Tashkun, S. A., Tennyson, J., Toon, G. C., Tyuterev V. G. and Wagner, G.: The HITRAN 2012 molecular spectroscopic database. J. Quant. Spectrosc. Rad. Trans. 130, 4-50, doi:10.1016/j. Jqsrt. 2013.07.002, 2013.

Schoeberl, M. R., Douglass, A. R., Hilsenrath, E., Bhartia, P. K., Beer, R., Waters, J. W., Gunson, M. R., Froidevaux, L., Gille, J. C., Barnett, J. J., Levelt, P. F., and DeCola, P.: Overview of the EOS Aura mission, IEEE Trans. Geosci. Remote Sens., 44, 1066–1074, 2006.

5   Schneider, M., Gonzàlez, Y., Dyroff, C., Christner, E., Wiegele, A., Barthlott, S., García, O. E., Sepûlveda, E., Hase, F., Andrey, J., Blumenstock, T., Guirado, C., Ramos, R., and Rodríguez, S.: Empirical validation and proof of added value of MUSICA's tropospheric δD remote sensing products, Atmos. Meas. Tech., 8, 483–503, doi:10.5194/amt-8-483-2015, 2015.

Schneider, M., Wiegele, A., Barthlott, S., Gonzàlez, Y., Christner, E., Dyroff, C., García, O. E., Hase, F., Blumenstock, T., Sepûlveda, E., Mengistu Tsidu, G., Takele Kenea, S., Rodríguez, S., and Andrey, J.: Accomplishments of the MUSICA project to provide accurate, long-term, global and high-resolution observations of tropospheric [H_2O; δD] pairs – a review, Atmos. Meas. Tech., 9, 2845–2875, doi:10.5194/amt-9-2845-2016, 2016

Solomon, S., Stratopheric Ozone depletion: A review of Concepts and History, Rev. Geophys., 37, 275-315, 1999.

Samuel, T. K.: Determination of Atmospheric Water Vapour Isotopic Composition using Multi-Platform Instruments and Models over Ethiopia: Implications for Water Cycle, PhD dissertation, Addis Ababa university, department of physics, 2014.

15   Sussmann, R., Forster, F., Rettinger, M., and Bousquet, P.: Renewed methane increase for five years (2007–2011) observed by solar FTIR spectrometry, Atmos. Chem. Phys., 12, 4885–4891, doi:10.5194/acp-12-4885-2012, 2012.

Sussmann, R., Forster, F., Rettinger, M., and Jones, N.: Strategy for high-accuracy-and-precision retrieval of atmospheric methane from the mid-infrared FTIR network, Atmos. Meas. Tech., 4, 1943-1964, doi:10.5194/amt-4-1943-2011, 2011.

Senten, C., De Mazière M., Dils B., Hermans C., Kruglanski M., Neefs E., Scolas F., C. Vandaele A., Vanhaelewyn G., Vigouroux C., Carleer M., F. Coheur P., Fally S., Barret B., L. Baray J., Delmas R., Leveau J., M. Metzger J., Mahieu E., Boone C., A. Walker K., F. Bernath P. and Strong K.; Technical Note: New ground-based FTIR measurements at Ile de LaRéunion: observations, error analysis, and comparisons with independent data; Atmos. Chem. Phys., 8, 3483–3508, 2008.

Stiller, G. P., Kiefer, M., Eckert, E., von Clarmann, T., Kellmann, S., García-Comas, M., Funke, B., Leblanc, T., Fetzer, E., Froidevaux, L., Gomez, M., Hall, E., Hurst, D., Jordan, A., Kämpfer, N., Lambert, A., McDermid, I. S., McGee, T., Miloshevich, L., Nedoluha, G., 25   Read, W., Schneider, M., Schwartz, M., Straub, C., Toon, G., Twigg, L. W., Walker, K., and Whiteman, D. N.: Validation of MIPAS IMK/IAA temperature, water vapor, and ozone profiles with MOHAVE-2009 campaign measurements, Atmos. Meas. Tech., 5, 289–320, doi:10.5194/amt-5-289-2012, 2012.

Sussmann, R., Borsdorff, T., Rettinger, M., Camy-Peyret, C., Demoulin, P., Duchatelet, P., Mahieu, E., and Servais, C.: Technical Note: Harmonized retrieval of column-integrated atmospheric water vapor from the FTIR network-first examples for long-term records and 30   station trends, Atmos. Chem. Phys., 9, 8987–8999, doi:10.5194/acp-9-8987-2009, 2009.

Tikhonov, A.: On the regularization of ill-posed problems, Dokl. Acad. Nauk SSSR, 153, 49–52, 1963b

Tilmes, S., Kinnison, D. E., Garcia, R. R., M¨uller, R., Sassi,F., Marsh, D. R., and Boville, B. A.: Evaluation of heterogeneous processes in the polar lower stratosphere in the Whole Atmosphere Community Climate Model, J. Geophys. Res., 112, D24301, doi:10.1029/2006JD008334, 2007

35   Takele Kenea, S., Mengistu Tsidu, G., Blumenstock, T., Hase, F., von Clarmann, T., and Stiller, G. P.: Retrieval and satellite intercomparison of O_3 measurements from ground-based FTIR Spectrometer at Equatorial Station: Addis Ababa, Ethiopia, Atmos. Meas. Tech., 6, 495-509, doi:10.5194/amt-6-495-2013, 2013.

von Clarmann, T.: Validation of remotely sensed profiles of atmospheric state variables: strategies and terminology, Atmos. Chem. Phys., 6, 4311–4320, doi:10.5194/acp-6-4311, 2006.

von Clarmann, T.: Smoothing error pitfalls, Atmos. Meas. Tech., 7, 30233034, doi:10.5194/amt-7-3023-2014, 2014.

Waters, J. W., Froidevaux, L., Harwood, R. S., Jarnot, R. F., Pickett, H. M., Read, W. G., Siegel, P. H., Cofield, R. E., Filipiak, M. J., Flower, D. A., Holden, J. R., Lau, G. K., Livesey, N. J., Manney, G. L., Pumphrey, H. C., Santee, M. L., Wu, D. L., Cuddy, D. T., Lay, R. R., Loo, M. S., Perun, V. S., Schwartz, M. J., Stek, P. C., Thurstans, R. P., Boyles, M. A., Chandra, K. M., Chavez, M. C., Chen, G.S., Chudasama, B. V., Dodge, R., Fuller, R. A., Girard, M. A., Jiang, J. H., Jiang, Y., Knosp, B. W., LaBelle, R. C., Lam, J. C., Lee, K. A., Miller, D., Oswald, J. E., Patel, N. C., Pukala, D. M., Quintero, O., Scaff, D. M., Snyder, W. V., Tope, M. C., Wagner, P. A., and Walch, M. J.: The Earth Observing System Microwave Limb Sounder (EOS MLS) on the Aura satellite, IEEE T. Geosci. Remote, 44, 1075–1092, doi:10.1109/tgrs.2006.873771, 2006.

WMO, Greenhouse Gas Bulletin, The State of Green house Gases in the Atmosphere Based on Global Observations through 2009, No. 6: 24 November 2010.

Xiong, X.Z., Barnet, C., Maddy, E., Sweeney, C., Liu, X. P., Zhou, L.H. and Goldberg, M.: Characterization and validation of methane products from the Atmospheric Infrared Sounder (AIRS), J. Geophys. Res. Biogeosci.113, doi:1410.1029/2007jg000500, 2008.

Xiong, X., Maddy, E. S., Barnet, C., Gambacorta, A., Patra, P. K., Sun, F. and Goldberg, M.: Retrieval of nitrous oxide from Atmospheric Infrared Sounder: Characterization and validation, J. Geophys. Res. Atmos., 119, 9107–9122, doi:10.1002/2013JD021406, 2014.